

PREPARED FOR THE U.S. DEPARTMENT OF ENERGY,
UNDER CONTRACT DE-AC02-76CH03073

PPPL-3940
UC-70

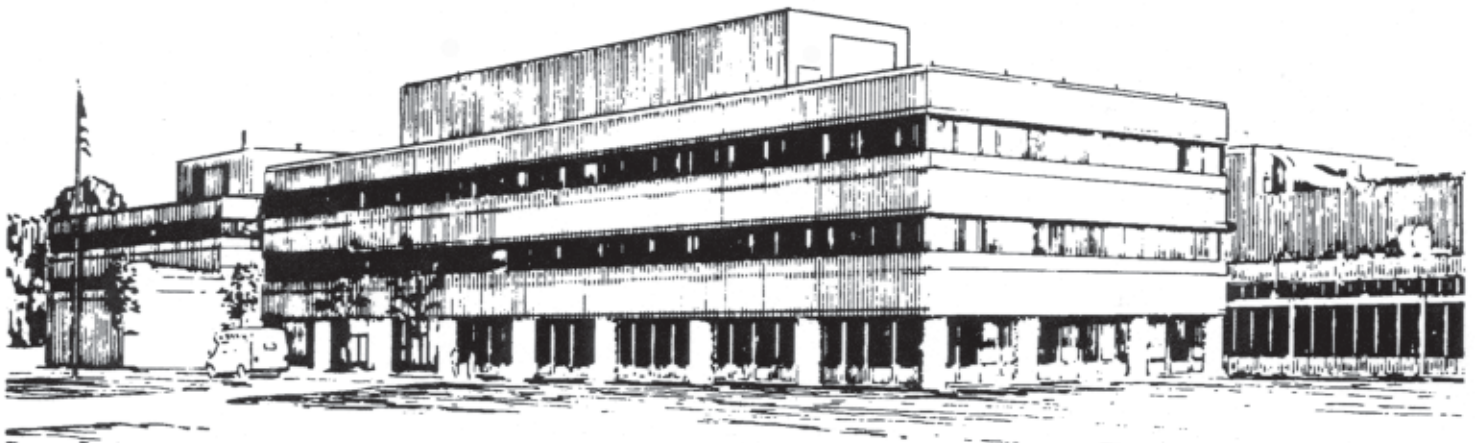
PPPL-3940

**Weibel and Two-stream Instabilities
for Intense Charged Particle Beam Propagation
through Neutralizing Background Plasma**

by

Ronald C. Davidson, Igor Kaganovich, and Edward A. Startsev

April 2004



**PRINCETON PLASMA PHYSICS LABORATORY
PRINCETON UNIVERSITY, PRINCETON, NEW JERSEY**

PPPL Reports Disclaimer

This report was prepared as an account of work sponsored by an agency of the United States Government. Neither the United States Government nor any agency thereof, nor any of their employees, makes any warranty, express or implied, or assumes any legal liability or responsibility for the accuracy, completeness, or usefulness of any information, apparatus, product, or process disclosed, or represents that its use would not infringe privately owned rights. Reference herein to any specific commercial product, process, or service by trade name, trademark, manufacturer, or otherwise, does not necessarily constitute or imply its endorsement, recommendation, or favoring by the United States Government or any agency thereof. The views and opinions of authors expressed herein do not necessarily state or reflect those of the United States Government or any agency thereof.

Availability

This report is posted on the U.S. Department of Energy's Princeton Plasma Physics Laboratory Publications and Reports web site in Fiscal Year 2004. The home page for PPPL Reports and Publications is: http://www.pppl.gov/pub_report/

DOE and DOE Contractors can obtain copies of this report from:

U.S. Department of Energy
Office of Scientific and Technical Information
DOE Technical Information Services (DTIS)
P.O. Box 62
Oak Ridge, TN 37831

Telephone: (865) 576-8401

Fax: (865) 576-5728

Email: reports@adonis.osti.gov

This report is available to the general public from:

National Technical Information Service
U.S. Department of Commerce
5285 Port Royal Road
Springfield, VA 22161

Telephone: 1-800-553-6847 or
(703) 605-6000

Fax: (703) 321-8547

Internet: <http://www.ntis.gov/ordering.htm>

Weibel and Two-Stream Instabilities for Intense Charged Particle Beam Propagation Through Neutralizing Background Plasma

Ronald C. Davidson, Igor Kaganovich, and Edward A. Startsev

Plasma Physics Laboratory

Princeton University

Princeton, NJ 08543

(Dated: May 10, 2004)

Properties of the multi-species electromagnetic Weibel and electrostatic two-stream instabilities are investigated for an intense ion beam propagating through background plasma. Assuming that the background plasma electrons provide complete charge and current neutralization, detailed linear stability properties are calculated within the framework of a macroscopic cold-fluid model for a wide range of system parameters.

I. INTRODUCTION

High energy ion accelerators, transport systems and storage rings [1–5] are used in fundamental high energy and nuclear physics research and for applications such as heavy ion fusion, spallation neutron sources, and nuclear waste transmutation. Charged particle beams are subject to various collective processes that can deteriorate the beam quality. Of particular importance at the high beam currents and charge densities of interest for heavy ion fusion are the effects of the intense self-fields produced by the beam space charge and current on determining detailed equilibrium, stability, and transport properties. In general, a complete description of collective processes in intense charged particle beams is provided by the nonlinear Vlasov-Maxwell equations [1] for the self-consistent evolution of the beam distribution function, $f_b(\mathbf{x}, \mathbf{p}, t)$, and the electric and magnetic fields, $\mathbf{E}(\mathbf{x}, t)$ and $\mathbf{B}(\mathbf{x}, t)$. While considerable progress has been made in analytical and numerical simulation studies of intense beam propagation [6–70], the effects of finite geometry and intense self-fields often make it difficult to obtain detailed predictions of beam equilibrium, stability, and transport properties based on the Vlasov-Maxwell equations. Nonetheless, often with the aid of numerical simulations, there has been considerable recent analytical progress in applying the Vlasov-Maxwell equations to investigate the detailed equilibrium and stability properties of intense charged particle beams. These investigations include a wide variety of collective interaction processes ranging from the electrostatic Harris instability [29–35] and electromagnetic Weibel instability [36–41] driven by large temperature anisotropy with $T_{\perp b} \gg T_{\parallel b}$ in a one-component nonneutral ion beam, to wall-impedance-driven collective instabilities [42–45], to the dipole-mode two-stream instability for an intense ion beam propagating through a partially neutralizing electron background [45–56], to the resistive hose instability [57–63] and the sausage and hollowing instabilities [64–66] for an intense ion beam propagating through a background plasma [67–70], to the development of a nonlinear stability theorem [20, 21] in the smooth-focusing approximation.

In the plasma plug and target chamber regions for heavy ion fusion, the intense ion beam experiences collective interactions with the background plasma. In this paper, we investigate theoretically properties of the multi-species electromagnetic Weibel and electrostatic two-stream instabilities for an intense ion beam propagating through background plasma. Assuming that the background plasma electrons provide complete charge and current neutralization, detailed linear stability properties are calculated within the framework of a macroscopic cold-fluid model for a wide range of system parameters.

The organization of this paper is the following. The assumptions and theoretical model are de-

scribed in Sec. II. The eigenvalue equations for the Weibel instability and the two-stream instability are then analyzed in Sec. III and IV, respectively.

II. MACROSCOPIC FLUID MODEL AND EIGENVALUE EQUATION

In the present analysis, we make use of a macroscopic fluid model [1, 71] to describe the interaction of an intense ion beam ($j = b$) with background plasma electrons and ions ($j = e, i$). The charge and rest mass of a particle of species j ($j = b, e, i$) are denoted by e_j and m_j , respectively. In equilibrium, the steady-state ($\partial/\partial t = 0$) average flow velocities are taken to be in the z -direction, $\mathbf{V}_j^0(\mathbf{x}) = V_{zj}^0(r)\hat{\mathbf{e}}_z = \beta_j(r)c\hat{\mathbf{e}}_z$, and cylindrical symmetry is assumed ($\partial/\partial\theta = 0$). Axial motions are generally allowed to be relativistic, and the directed axial kinetic energy is denoted by $(\gamma_j - 1)m_jc^2$, where $\gamma_j(r) = [1 - \beta_j^2(r)]^{-1/2}$ is the relativistic mass factor of a fluid element. Furthermore, the analysis is carried out in the paraxial approximation, treating the velocity spread of the beam particles as small in comparison with $\beta_b c$. Denoting the equilibrium density profile by $n_j^0(r)$ ($j = b, e, i$), the corresponding equilibrium self-electric field, $\mathbf{E}^0(\mathbf{x}) = E_r^0(r)\hat{\mathbf{e}}_r$, and azimuthal self-magnetic field, $\mathbf{B}^0(\mathbf{x}) = B_\theta^0(r)\hat{\mathbf{e}}_\theta$, are determined self-consistently from

$$\frac{1}{r} \frac{\partial}{\partial r} r \frac{\partial}{\partial r} E_r^0(r) = \sum_{j=b,e,i} 4\pi e_j n_j^0(r) , \quad (1)$$

$$\frac{1}{r} \frac{\partial}{\partial r} r \frac{\partial}{\partial r} B_\theta^0(r) = \sum_{b,e,i} 4\pi e_j \beta_j(r) n_j^0(r) , \quad (2)$$

where $r = (x^2 + y^2)^{1/2}$ is the radial distance from the axis of symmetry. Finally, denoting the transverse pressure by $P_{\perp j}^0(r) = n_j^0(r)T_{\perp j}^0(r)$, equilibrium radial force balance on a fluid element of species j corresponding to a self-pinch equilibrium is given by

$$\frac{\partial}{\partial r} P_{\perp j}^0(r) = n_j^0(r) e_j [E_r^0(r) - \beta_j(r) B_\theta^0(r)] . \quad (3)$$

Examples of specific equilibrium profiles consistent with Eqs. (1)–(3) are given in Chapter 10 of Ref. 1.

In the macroscopic stability analysis, we specialize to the case of axisymmetric, electromagnetic perturbations with $\partial/\partial\theta = 0$ and $\partial/\partial z = 0$, and perturbed quantities are expressed as $\delta\psi(r, t) = \delta\psi(r)\exp(-i\omega t)$ where $Im\omega > 0$ corresponds to instability (temporal growth). For the perturbations, the perturbed field components are $\delta\mathbf{E}(\mathbf{x}, t) = \delta E_r(r, t)\hat{\mathbf{e}}_r + \delta E_z(r, t)\hat{\mathbf{e}}_z$ and $\delta\mathbf{B}(\mathbf{x}, t) = \delta B_\theta(r, t)\hat{\mathbf{e}}_\theta$, where

$$-\frac{i\omega}{c}\delta B_\theta(r) = \frac{\partial}{\partial r}\delta E_z(r) \quad (4)$$

follows from the θ -component of the $\nabla \times \delta \mathbf{E}$ Maxwell equation. Furthermore, some straightforward algebra shows that the r and z -components of the $\nabla \times \delta \mathbf{B}$ Maxwell equation can be expressed as

$$\left(\frac{1}{r} \frac{\partial}{\partial r} r \frac{\partial}{\partial r} + \frac{\omega^2}{c^2} \right) \delta E_z(r) = -\frac{4\pi i \omega}{c^2} \left(\sum_{j=b,e,i} e_j n_j^0(r) \delta V_{zj}(r) + \sum_{j=b,e,i} e_j \beta_j(r) c \delta n_j(r) \right), \quad (5)$$

$$\frac{\omega^2}{c^2} \delta E_r(r) = -\frac{4\pi i \omega}{c^2} \sum_{j=b,e,i} e_j n_j^0(r) \delta V_{rj}(r), \quad (6)$$

where δV_{zj} , δV_{rj} and δn_j are determined self-consistently in terms of δE_z from the linearized continuity and force-balance equations. Note from Eqs. (4)-(6) that the field perturbations have mixed polarization with both a longitudinal component ($\delta E_r \neq 0$) and transverse electromagnetic field components ($\delta B_\theta \neq 0$ and $\delta E_z \neq 0$). This is because for drifting charge components with $\beta_j \neq 0$ the electrostatic and ordinary-mode electromagnetic perturbations are coupled.

With regard to the linearized continuity and force balance equations, in the present macroscopic analysis we neglect the effects of pressure perturbations. Denoting the density and average momentum of a fluid element of species j by $n_j = n_j^0 + \delta n_j$ and $\mathbf{P}_j = \gamma_j m_j \beta_j c \hat{\mathbf{e}}_z + \delta \mathbf{P}_j$, respectively, the linearized continuity and force balance equations can be expressed as

$$-i\omega \delta n_j + \frac{1}{r} \frac{\partial}{\partial r} (r n_j^0 \delta V_{rj}) = 0, \quad (7)$$

$$-i\omega \delta P_{rj} = -e_j \left(\delta E_r + \frac{1}{c} \delta V_{zj} B_\theta^0 + \beta_j \delta B_\theta \right), \quad (8)$$

$$-i\omega \delta P_{zj} = e_j \left(\delta E_z + \frac{1}{c} \delta V_{rj} B_\theta^0 \right), \quad (9)$$

where $\delta P_{\theta j} = 0$ and $\beta_j(r)c = V_{zj}^0(r)$. Here, we can express $\delta \mathbf{P}_j = \gamma_j m_j \delta \mathbf{V}_j + \delta \gamma_j m_j \beta_j c \hat{\mathbf{e}}_z$, where $\delta \gamma_j = (\gamma_j^3/c^2) \mathbf{V}_j^0 \cdot \delta \mathbf{V}_j = (\gamma_j^3/c) \beta_j \delta V_{zj}$ and $\gamma_j = (1 - \beta_j^2)^{-1/2}$, which gives the expected results $\delta P_{rj} = \gamma_j m_j \delta V_{rj}$ and $\delta P_{zj} = \gamma_j^3 m_j \delta V_{zj}$.

It has been shown previously that a sufficiently strong self-magnetic field $B_\theta^0 \neq 0$ tends to reduce the growth rate of the Weibel instability in intense beam-plasma systems [72]. For our purposes here, in the remainder of this paper we specialize to the case of a charge-neutralized and current-neutralized beam-plasma system with

$$\sum_{j=b,e,i} n_j^0(r) e_j = 0, \quad \sum_{j=b,e,i} n_j^0(r) \beta_j e_j = 0, \quad (10)$$

where β_j is taken to be independent of r for simplicity. It then follows from Eqs. (1), (2) and (10) that $E_r^0 = 0 = B_\theta^0$, which is consistent with Eq. (3) in the cold-fluid limit. Setting $B_\theta^0(r) = 0$ in Eqs. (5)–(9) gives

$$i\omega\delta V_{rj} = -\frac{e_j}{\gamma_j m_j} \left(\delta E_r - \frac{ic\beta_j}{\omega} \frac{\partial}{\partial r} \delta E_z \right), \quad (11)$$

$$i\omega\delta V_{zj} = -\frac{e_j}{\gamma_j^3 m_j} \delta E_z, \quad (12)$$

for the perturbed flow velocities. Combining Eqs. (4), (6) and (11) then gives

$$\left[\omega^2 - \sum_{j=b,e,i} \omega_{pj}^2(r) \right] \delta E_r = -\frac{ic}{\omega} \left(\sum_{j=b,e,i} \beta_j \omega_{pj}^2(r) \right) \frac{\partial}{\partial r} \delta E_z, \quad (13)$$

where $\omega_{pj}^2(r) = 4\pi n_j^0(r) e_j^2 / \gamma_j m_j$ is the relativistic plasma frequency-squared. Note that Eq. (13) relates the longitudinal electric field δE_r directly to $(\partial/\partial r)\delta E_z$. It is clear from Eq. (13) that $\delta E_r \neq 0$ whenever $\sum_{j=b,e,i} \beta_j \omega_{pj}^2 \neq 0$. From Eqs. (4), (11) and (13), we then obtain for the perturbed radial flow velocity

$$-i\omega\gamma_j m_j \delta V_{rj} = -e_j \left[\beta_j + \frac{\sum_{j=b,e,i} \beta_j \omega_{pj}^2(r)}{\omega^2 - \sum_{j=b,e,i} \omega_{pj}^2(r)} \right] \frac{ic}{\omega} \frac{\partial}{\partial r} \delta E_z. \quad (14)$$

Making use of Eqs. (7), (12) and (14) to express δV_{zj} and δn_j directly in terms of δE_z and $(\partial/\partial r)\delta E_z$, some straightforward algebra shows that the Maxwell equation (5) can be expressed as

$$\frac{1}{r} \frac{\partial}{\partial r} \left[r \left(1 + \sum_{j=b,e,i} \frac{\beta_j^2 \omega_{pj}^2(r)}{\omega^2} + \frac{(\sum_{j=b,e,i} \beta_j \omega_{pj}^2(r))^2}{\omega^2 - \sum_{j=b,e,i} \omega_{pj}^2(r)} \right) \frac{\partial}{\partial r} \delta E_z \right] + \left(\frac{\omega^2}{c^2} - \sum_{j=b,e,i} \frac{\omega_{pj}^2(r)}{\gamma_j^2 c^2} \right) \delta E_z = 0, \quad (15)$$

where $\gamma_j = (1 - \beta_j^2)^{-1/2}$ is the relativistic mass factor, and $\omega_{pj}^2(r) = 4\pi n_j^0(r) e_j^2 / \gamma_j m_j$.

Equation (15) is the desired eigenvalue equation for axisymmetric, electromagnetic perturbations with polarization $\delta \mathbf{E} = \delta E_r \hat{\mathbf{e}}_r + \delta E_z \hat{\mathbf{e}}_z$ and $\delta \mathbf{B} = \delta B_\theta \hat{\mathbf{e}}_\theta$, with the terms proportional to $\sum_{j=b,e,i} \beta_j^2 \omega_{pj}^2(r)$ and $\sum_{j=b,e,i} \beta_j \omega_{pj}^2(r)$ providing the free energy to drive the Weibel instability. Equation (15) can be integrated numerically to determine the eigenvalue ω^2 and eigenfunction $\delta E_z(r)$ for a wide range of beam-plasma density profiles $n_j^0(r)$. As discussed in Sec. III, analytical solutions are also tractable for the case of flat-top (step-function) density profiles. As a general remark, when $\sum_{j=b,e,i} \beta_j^2 \omega_{pj}^2(r) \neq 0$ and $\sum_{j=b,e,i} \beta_j \omega_{pj}^2(r) \neq 0$, Eq. (15) supports both stable fast-wave solutions ($Im\omega = 0$, $|\omega/ck_\perp| > 1$) and unstable slow-wave solutions ($Im\omega > 0$, $|\omega/ck_\perp| < 1$). Here, $|k_\perp| \sim |\partial/\partial r|$ is the characteristic radial wavenumber of the perturbation. Moreover, Eq. (15) also supports stable plasma oscillation solutions with predominantly longitudinal polarization associated with the factor proportional to $[\omega^2 - \sum_{j=b,e,i} \omega_{pj}^2(r)]^{-1}$. Finally, for a perfectly conducting

cylindrical wall located at $r = r_w$, the eigenvalue equation (15) is to be solved subject to the boundary condition

$$\delta E_z(r = r_w) = 0 . \quad (16)$$

III. WEIBEL INSTABILITY FOR STEP-FUNCTION DENSITY PROFILES

As an example that is analytically tractable, we consider the case illustrated in Fig. 1 where the density profiles are uniform both inside and outside the beam with

$$n_j^0(r) = \hat{n}_j^i = \text{const.}, \quad j = b, e, i , \quad (17)$$

for $0 \leq r < r_b$, and

$$n_j^0(r) = \hat{n}_j^o = \text{const.}, \quad j = e, i , \quad (18)$$

for $r_b < r \leq r_w$. Here, the superscript “i” (“o”) denotes inside (outside) the beam, and $\hat{n}_b^o = 0$ is assumed. Consistent with Eq. (10), $\sum_{j=b,e,i} \hat{n}_j^i e_j = 0 = \sum_{j=b,e,i} \hat{n}_j^o \beta_j e_j$ and $\sum_{j=e,i} \hat{n}_j^o e_j = 0 = \sum_{j=e,i} \hat{n}_j^o \beta_j e_j$ are assumed. We also take $\beta_j = 0$ ($j = e, i$) in the region outside the beam ($r_b < r \leq r_w$). The subsequent analysis of the eigenvalue equation (15) is able to treat the three cases: (a) beam-plasma-filled waveguide ($r_b = r_w$); (b) vacuum region outside the beam ($r_b < r_w$ and $\hat{n}_j^o = 0$, $j = e, i$); and (c) plasma outside the beam ($r_b < r_w$ and $\hat{n}_j^o \neq 0$, $j = e, i$).

Referring to Fig. 1 and Eq. (15), it is convenient to introduce the constant coefficients

$$T_i^2(\omega) = \left[\frac{\omega^2}{c^2} - \sum_{j=b,e,i} \frac{\hat{\omega}_{pj}^{i2}}{\gamma_j^2 c^2} \right] \times \left[1 + \sum_{j=b,e,i} \frac{\beta_j^2 \hat{\omega}_{pj}^{i2}}{\omega^2} + \frac{(\sum_{j=b,e,i} \beta_j \hat{\omega}_{pj}^{i2})^2}{\omega^2 [\omega^2 - \sum_{j=b,e,i} \hat{\omega}_{pj}^{i2}] } \right]^{-1} \quad (19)$$

for $0 \leq r < r_b$, and

$$T_0^2(\omega) = - \left[\frac{\omega^2}{c^2} - \sum_{j=e,i} \frac{\hat{\omega}_{pj}^{o2}}{c^2} \right] \quad (20)$$

for $r_b < r \leq r_w$, where $\hat{\omega}_{pj}^{i2} = 4\pi \hat{n}_j^i e_j^2 / \gamma_j m_j$, $j = b, e, i$, and $\hat{\omega}_{pj}^{o2} = 4\pi \hat{n}_j^o e_j^2 / m_j$, $j = e, i$. We denote the eigenfunction inside the beam ($0 \leq r < r_b$) by $\delta E_z^I(r)$ and the eigenfunction outside the beam ($r_b < r \leq r_w$) by $\delta E_z^{II}(r)$. Equations (15), (19) and (20) then give

$$\frac{1}{r} \frac{\partial}{\partial r} r \frac{\partial}{\partial r} \delta E_z^I + T_i^2 \delta E_z^I = 0 , \quad 0 \leq r < r_b , \quad (21)$$

and

$$\frac{1}{r} \frac{\partial}{\partial r} r \frac{\partial}{\partial r} \delta E_z^{II} - T_0^2 \delta E_z^{II} = 0 , \quad r_b < r \leq r_w . \quad (22)$$

in the two regions. Equations (21) and (22) are Bessel's equations of order zero. The solutions to Eqs. (21) and (22) that are regular at $r = 0$, continuous at $r = r_b$, and vanish at the conducting wall are given by

$$\delta E_z^I(r) = AJ_0(T_i r), \quad 0 \leq r < r_b, \quad (23)$$

$$\delta E_z^{II}(r) = AJ_0(T_i r_b) \frac{K_0(T_0 r_w) I_0(T_0 r) - K_0(T_0 r) I_0(T_0 r_w)}{K_0(T_0 r_w) I_0(T_0 r_b) - K_0(T_0 r_b) I_0(T_0 r_w)}, \quad r_b < r \leq r_w, \quad (24)$$

where A is a constant, $J_0(x)$ is the Bessel function of the first kind of order zero, and $I_0(x)$ and $K_0(x)$ are modified Bessel functions of order zero.

The remaining boundary condition is obtained by integrating the eigenvalue equation (15) across the beam surface at $r = r_b$. Making use of Eqs. (17) and (18), and assuming $\beta_e = 0 = \beta_i$ in the region outside the beam ($r_b < r \leq r_w$), we operate on Eq. (14) with $\int_{r_b(1-\epsilon)}^{r_b(1+\epsilon)} dr \dots$ for $\epsilon \rightarrow 0_+$. This readily gives the boundary condition

$$\left(1 + \sum_{j=b,e,i} \frac{\beta_j^2 \hat{\omega}_{pj}^2}{\omega^2} + \frac{(\sum_{j=b,e,i} \beta_j \hat{\omega}_{pj}^2)^2}{\omega^2 [\omega^2 - \sum_{j=b,e,i} \hat{\omega}_{pj}^2]} \right) \left[\frac{\partial}{\partial r} \delta E_z^I \right]_{r=r_b} = \left[\frac{\partial}{\partial r} \delta E_z^{II} \right]_{r=r_b}, \quad (25)$$

which relates the change in $\delta B_\theta = (ic/\omega)(\partial \delta E_z / \partial r)$ at $r = r_b$ to the perturbed surface current. Substituting Eqs. (23) and (24) into Eq. (25) then gives

$$\begin{aligned} & \left(1 + \sum_{j=b,e,i} \frac{\beta_j^2 \hat{\omega}_{pj}^2}{\omega^2} + \frac{(\sum_{j=b,e,i} \beta_j \hat{\omega}_{pj}^2)^2}{\omega^2 [\omega^2 - \sum_{j=b,e,i} \hat{\omega}_{pj}^2]} \right) T_i r_b \frac{J_0'(T_i r_b)}{J_0(T_i r_b)} \\ & = T_0 r_b \frac{K_0(T_0 r_w) I_0'(T_0 r_b) - K_0'(T_0 r_b) I_0(T_0 r_w)}{K_0(T_0 r_w) I_0(T_0 r_b) - K_0(T_0 r_b) I_0(T_0 r_w)}, \end{aligned} \quad (26)$$

where $T_i(\omega)$ and $T_0(\omega)$ are defined in Eqs. (19) and (20), and $I_0'(x) = (d/dx)I_0(x)$, $J_0'(x) = -(d/dx)J_0(x)$, etc.

Equation (26) constitutes a closed transcendental dispersion relation that determines the complex oscillation frequency ω for electromagnetic perturbations about the step-function profiles in Eqs. (17) and (18). As noted earlier, the dispersion relation has both fast-wave and slow-wave (Weibel-type) solutions, as well as a predominantly longitudinal (modified plasma oscillation) solution, and can be applied to the case of a beam-plasma-filled waveguide, or to the case where the region outside the beam ($r_b < r \leq r_w$) corresponds to vacuum ($\hat{n}_j^0 = 0, j = e, i$) or background plasma ($\hat{n}_j^0 \neq 0, j = e, i$).

A. Beam-Plasma-Filled Waveguide ($r_b = r_w$)

For the case where the beam-plasma system extends to the conducting wall ($r_b = r_w$), the solution $\delta E_z^I(r) = AJ_0(T_i r)$ in Eq. (23) is applicable over the entire interval $0 \leq r \leq r_w$. Applying the boundary condition $\delta E_z^I(r = r_w) = 0$ then gives the dispersion relation

$$J_0(T_i r_w) = 0, \quad (27)$$

which also follows from Eq. (26) in the limit $r_b \rightarrow r_w$. We denote by p_{on} the n 'th zero of $J_0(p_{on}) = 0$, and introduce the effective perpendicular wavenumber (quantized) defined by $k_\perp^2 = p_{on}^2/r_w^2$, $n = 1, 2, \dots$. The solutions to Eq. (27) are then determined from

$$T_i^2(\omega) = k_\perp^2, \quad n = 1, 2, \dots, \quad (28)$$

or equivalently,

$$1 + \sum_{j=b,e,i} \frac{\beta_j^2 \hat{\omega}_{pj}^2}{\omega^2} + \frac{(\sum_{j=b,e,i} \beta_j \hat{\omega}_{pj}^2)^2}{\omega^2 [\omega^2 - \sum_{j=b,e,i} \hat{\omega}_{pj}^2]} = \frac{\omega^2}{c^2 k_\perp^2} - \sum_{j=b,e,i} \frac{\hat{\omega}_{pj}^2}{\gamma_j^2 c^2 k_\perp^2}, \quad (29)$$

where use has been made of Eq. (19). In the absence of axial flow ($\beta_j = 0, j = b, e, i$), note that the solution to Eq. (29) leads to the familiar fast-wave solution $\omega^2 = c^2 k_\perp^2 + \sum_{j=b,e,i} \omega_{pj}^2$ with $\gamma_j = 1$. For $\sum_j \beta_j^2 \hat{\omega}_{pj}^2 \neq 0$ and $\sum_j \beta_j \hat{\omega}_{pj}^2 \neq 0$, however, Eq. (29) supports two other solutions corresponding to the Weibel instability and plasma oscillation solution.

Equation (29) is a cubic equation for ω^2 . It is convenient to introduce the dimensionless quantities Ω^2 , K_\perp^2 , $\langle \beta^2 \rangle$ and $\langle \beta \rangle$ defined by

$$\begin{aligned} \Omega^2 &= \frac{\omega^2}{\sum_{j=b,e,i} \hat{\omega}_{pj}^2}, & K_\perp^2 &= \frac{c^2 k_\perp^2}{\sum_{j=b,e,i} \hat{\omega}_{pj}^2}, \\ \langle \beta^2 \rangle &= \frac{\sum_{j=b,e,i} \beta_j^2 \hat{\omega}_{pj}^2}{\sum_{j=b,e,i} \hat{\omega}_{pj}^2}, & \langle \beta \rangle &= \frac{\sum_{j=b,e,i} \beta_j \hat{\omega}_{pj}^2}{\sum_{j=b,e,i} \hat{\omega}_{pj}^2}. \end{aligned} \quad (30)$$

Rearranging terms, the dispersion relation (29) for a beam-plasma-filled waveguide can be expressed as

$$K_\perp^2 [\Omega^4 - \Omega^2(1 - \langle \beta^2 \rangle) + (\langle \beta \rangle^2 - \langle \beta^2 \rangle)] = [\Omega^2 - (1 - \langle \beta^2 \rangle)] \Omega^2 (\Omega^2 - 1), \quad (31)$$

where use has been made of $\sum_{j=b,e,i} \hat{\omega}_{pj}^2 / \gamma_j^2 = (1 - \langle \beta^2 \rangle) \sum_{j=b,e,i} \hat{\omega}_{pj}^2$. In the absence of axial streaming ($\beta_j = 0$ and $\langle \beta \rangle = 0 = \langle \beta^2 \rangle$), the dispersion relation (31) gives directly the fast wave solution, $\Omega^2 = 1 + K_\perp^2$, or equivalently, $\omega^2 = c^2 k_\perp^2 + \sum_{j=b,e,i} \hat{\omega}_{pj}^2$, as expected. On the other

hand, for $\langle\beta^2\rangle \neq 0$ and $\langle\beta\rangle \neq 0$, and sufficiently short-wavelength perturbations that $K_{\perp}^2 = c^2 k_{\perp}^2 / \sum_{j=b,e,i} \hat{\omega}_{pj}^2 \gg 1$, the dispersion relation (31) can be approximated by

$$\Omega^4 - \Omega^2(1 - \langle\beta^2\rangle) - (\langle\beta^2\rangle - \langle\beta\rangle^2) = 0. \quad (32)$$

The solutions to the quadratic equation (32) for Ω^2 are given by

$$\Omega^2 = \frac{1}{2}(1 - \langle\beta^2\rangle) \left[1 \pm \left(1 + \frac{4(\langle\beta^2\rangle - \langle\beta\rangle^2)}{(1 - \langle\beta^2\rangle)^2} \right)^{1/2} \right]. \quad (33)$$

It is readily shown from the definitions in Eq. (30) that $\langle\beta^2\rangle \geq \langle\beta\rangle^2$. Therefore the upper sign in Eq. (33) corresponds to stable plasma oscillations ($\Omega^2 > 0$) modified by axial streaming effects. On the other hand, for $\langle\beta^2\rangle > \langle\beta\rangle^2$ the lower sign in Eq. (33) corresponds to $\Omega^2 < 0$. Because $\Omega^2 < 0$ for the lower sign in Eq. (33), it follows that $Re\Omega = 0$ and

$$Im\Omega = \pm \frac{1}{\sqrt{2}}(1 - \langle\beta^2\rangle)^{1/2} \left[\left(1 + \frac{4(\langle\beta^2\rangle - \langle\beta\rangle^2)}{(1 - \langle\beta^2\rangle)^2} \right)^{1/2} - 1 \right]^{1/2}. \quad (34)$$

The upper sign in Eq. (34) corresponds to temporal growth (Weibel instability) with $Im\Omega > 0$. Whenever the inequality

$$\frac{4(\langle\beta^2\rangle - \langle\beta\rangle^2)}{(1 - \langle\beta^2\rangle)^2} \ll 1 \quad (35)$$

is satisfied, note that the growth rate for the unstable (upper) branch in Eq. (34) is given approximately by

$$Im\Omega = \frac{[\langle\beta^2\rangle - \langle\beta\rangle^2]^{1/2}}{(1 - \langle\beta^2\rangle)^{1/2}}. \quad (36)$$

In dimensional units, when the inequality in Eq. (35) is satisfied it follows from Eqs. (30) and (36) that the growth rate of the Weibel instability for short-wavelength perturbations ($c^2 k_{\perp}^2 \gg \sum_{j=b,e,i} \hat{\omega}_{pj}^2$) in a beam-plasma-filled waveguide can be approximated by

$$Im\omega \simeq \Gamma_w \equiv \frac{[\langle\beta^2\rangle - \langle\beta\rangle^2]^{1/2}}{(1 - \langle\beta^2\rangle)^{1/2}} \left(\sum_{j=b,e,i} \hat{\omega}_{pj}^2 \right)^{1/2}. \quad (37)$$

The quantity Γ_w defined in Eq. (37) provides a convenient unit in which to measure the growth rate of the Weibel instability in the subsequent numerical analysis of the general dispersion relation (26).

For a beam-plasma-filled waveguide, the exact solutions for ω^2 (or Ω^2) are of course determined from the cubic dispersion relation (29), or equivalently Eq. (31). With regard to the Weibel instability growth rate estimate in Eq. (36) or Eq. (37), it is important to recognize the relative size

of the contributions from the various beam-plasma species to the instability drive terms in Eq. (37). For present purposes, we consider a positively charged ion beam ($j = b$) propagating through background plasma electrons and ions ($j = e, i$). The charge states are denoted by $e_b = +Z_b e$, $e_e = -e$, and $e_i = +Z_i e$, and the plasma electrons are assumed to carry the neutralizing current ($\beta_e \neq 0$), whereas the plasma ions are taken to be stationary ($\beta_i = 0$). The conditions for charge neutralization, $\sum_{j=b,e,i} \hat{n}_j^i e_j = 0$, and current neutralization, $\sum_{j=b,e,i} \hat{n}_j^i e_j \beta_j = 0$, then give

$$\begin{aligned} \hat{n}_e^i &= Z_b \hat{n}_b^i + Z_i \hat{n}_i^i, \\ \beta_e &= \frac{\beta_b Z_b \hat{n}_b^i}{Z_b \hat{n}_b^i + Z_i \hat{n}_i^i}. \end{aligned} \quad (38)$$

Except for the case of a very tenuous beam ($Z_b \hat{n}_b^i \ll Z_i \hat{n}_i^i$), note from Eq. (38) that β_e can be a substantial fraction of β_b .

In the subsequent analysis of the dispersion relations (26) and (29), it is useful to define

$$\Omega_p^{i2} \equiv \sum_{j=b,e,i} \hat{\omega}_{pj}^{i2}, \quad \Omega_p^{02} \equiv \sum_{j=e,i} \hat{\omega}_{pj}^{02}, \quad (39)$$

where $\hat{\omega}_{pj}^{i2} = 4\pi \hat{n}_j^i e_j^2 / \gamma_j m_j$, $\gamma_j = (1 - \beta_j^2)^{-1/2}$ and $\hat{\omega}_{pj}^{02} = 4\pi \hat{n}_j^i e_j^2 / m_j$. Note from Eqs. (30) and (39) that $\sum_{j=b,e,i} \hat{\omega}_{pj}^{i2} / \gamma_j^2 = \Omega_p^{i2} - \langle \beta^2 \rangle \Omega_p^{i2}$. Careful examination of the expression for Γ_w in Eq. (37) for $\beta_i = 0$ shows that

$$\Gamma_w^2 = \frac{1}{(1 - \langle \beta^2 \rangle)} \left[\frac{(\beta_e^2 \hat{\omega}_{pe}^{i2} + \beta_b^2 \hat{\omega}_{pb}^{i2}) \hat{\omega}_{pi}^{i2} + (\beta_b - \beta_e)^2 \hat{\omega}_{pe}^{i2} \hat{\omega}_{pb}^{i2}}{\sum_{j=b,e,i} \hat{\omega}_{pj}^{i2}} \right]. \quad (40)$$

For $\hat{\omega}_{pb}^{i2}, \hat{\omega}_{pi}^{i2} \ll \hat{\omega}_{pe}^{i2}$, it follows that Eq. (40) is given to good approximation by

$$\Gamma_w^2 \simeq \frac{1}{(1 - \beta_e^2)} [\beta_e^2 \hat{\omega}_{pi}^{i2} + (\beta_b - \beta_e)^2 \hat{\omega}_{pb}^{i2}]. \quad (41)$$

Note from Eq. (41) that Γ_w involves the (slow) plasma frequencies of both the beam ions and the plasma ions.

In the remainder of Sec. III we consider the case of a cesium ion beam with $Z_b = 1$ and $\beta_b = 0.2$ propagating through a neutralizing background argon plasma with $Z_i = 1$, $\hat{n}_i^i = (1/2) \hat{n}_e^i = \hat{n}_b^i$, and $\beta_e = 0.1$ [see Eq. (38)]. Illustrative stability results obtained from Eq. (26) are shown in Figs. 2–5 for the case of a beam-plasma-filled waveguide, where the exact dispersion relation assumes the simple form in Eq. (29) with $k_\perp^2 = p_{on}^2 / r_w^2$, $n = 1, 2, \dots$, and $J_0(p_{on}) = 0$. In particular, Figs. 2 and 4 show plots of the normalized growth rate $(Im\omega) / \Gamma_w$ for the unstable branch versus radial mode number n for the choice of parameters corresponding to $\Omega_p^i r_b / c = 1/3$ (Fig. 2) and $\Omega_p^i r_b / c = 3$ (Fig. 4). The corresponding plots of the radial eigenfunction $\delta E_z(r)$ versus r/r_w are also shown

for mode number $n = 5$. Comparing Figs. 2 and 4, we note that the normalized growth rate for small values of n tends to be smaller for larger values of $\Omega_p^i r_b/c$. In general, for sufficiently large n , the instability growth rate asymptotes at $Im\omega \simeq \Gamma_w$, as expected from the estimate in Eq. (37). Figures 3 and 5 show plots of the normalized real frequency $(Re\omega)/\Omega_p^i$ versus radial mode number n obtained from Eq. (26) for the stable fast-wave branch. The system parameters in Figs. 3 and 5 are identical to those in Figs. 2 and 4, respectively, with $\Omega_p^i r_b/c = 1/3$ in Fig. 3, and $\Omega_p^i r_b/c = 3$ in Fig. 5. In both cases, as expected, $(Re\omega)/\Omega_p^i$ asymptotes at ck_\perp/Ω_p^i for large values of n , where $k_\perp^2 = p_{on}^2/r_w^2$.

B. Vacuum Region Outside of Beam-Plasma Channel ($r_b < r_w$; $\hat{n}_j^0 = 0, j = e, i$).

We now consider the case where there is a vacuum region outside the beam-plasma channel, i.e., $r_b < r_w$ and $\hat{n}_j^0 = 0, j = e, i$. In this case $T_0^2(\omega) = -\omega^2/c^2$ and $\Omega_p^{02} = 0$ follow from Eqs. (20) and (41), and the full transcendental dispersion relation (26) must be solved numerically. As before, both stable (fast-wave and plasma oscillation) and unstable (Weibel-like) solutions are found. For brevity, we focus here on the unstable solutions to Eq. (26). Typical numerical solutions to Eq. (26) are illustrated in Figs. 6 and 7 for the choice of system parameters $r_w = 3r_b$, $\beta_b = 0.2$, $\beta_e = 0.1$, $\hat{n}_i^i = \hat{n}_e^i/2 = \hat{n}_b^i$, $\Omega_p^0 = 0$ and $\Omega_p^i r_b/c = 1/3$ (Fig. 6) and $\Omega_p^i r_b/c = 3$ (Fig. 7). Shown in Figs. 6 and 7 are plots of the normalized growth rate $(Im\omega)/\Gamma_w$ versus radial mode number n , and plots of the eigenfunction $\delta E_z(r)$ versus r/r_w for mode number $n = 5$. Note from Figs. 6 and 7 that the signature of the instability growth rate for the case of a vacuum region outside the beam-plasma channel is qualitatively similar to that in Figs. 2 and 4 for the case of a beam-plasma-filled waveguide. However, the normalized growth rate in Fig. 7 is somewhat larger for lower values of radial mode number n than that in Fig. 4.

C. Plasma Outside of Beam-Plasma Channel ($r_b < r_w$; $\hat{n}_j^0 \neq 0, j = e, i$)

We now consider the dispersion relation (26) for the case where there is plasma outside the beam-plasma channel, i.e., $r_b < r_w$ and $\hat{n}_j^0 \neq 0, j = e, i$. In this case $T_0^2(\omega) = -(\omega^2/c^2 - \Omega_p^{02}/c^2)$, where $\Omega_p^{02} = \sum_{j=e,i} \hat{\omega}_{pj}^{02}$. Typical numerical solutions to Eq. (26) for the unstable branch are illustrated in Figs. 8 and 9 for the choice of system parameters $r_w = 3r_b$, $\beta_b = 0.2$, $\beta_e = 0.1$, $\hat{n}_i^i = \hat{n}_e^i/2 = \hat{n}_b^i = \hat{n}_e^o = \hat{n}_i^o$, and $\Omega_p^i r_b/c = 1/3$ (Fig. 8) and $\Omega_p^i r_b/c = 3$ (Fig. 9). Shown in Figs. 8 and 9 are plots of the normalized growth rate $(Im\omega)/\Gamma_w$ versus radial mode number n , and plots

of the eigenfunction $\delta E_z(r)$ versus r/r_w for mode number $n = 5$. Comparing Fig. 6 with Fig. 8, and Fig. 7 with Fig. 9, it is evident that the inclusion of plasma outside the beam-plasma channel does not significantly change the instability growth rate relative to the case where there is vacuum outside the beam-plasma channel.

To summarize, it is clear from the analysis in Sec. III that the Weibel instability with characteristic growth rate Γ_w can be particularly virulent for an intense ion charge bunch propagating through background plasma that provides full charge and current neutralization. It is therefore important to assess the relative importance of the electrostatic two-stream and electromagnetic Weibel instabilities for similar system parameters. This is briefly discussed in Sec. IV.

IV. ELECTROSTATIC TWO-STREAM INSTABILITY

In this section, for purposes of comparison with the Weibel instability, we present a brief discussion of the electrostatic two-stream instability for an intense ion beam pulse propagating through a background plasma. Similar to Secs. II and III, it is assumed that the beam-plasma system is fully charge neutralized and current neutralized [Eq. (10)] with $E_r^0(r) = 0 = B_\theta^0(r)$. Furthermore, attention is restricted to azimuthally symmetric ($\partial/\partial\theta = 0$) electrostatic perturbations with $\delta\mathbf{E}(\mathbf{x}, t) \simeq -\nabla\delta\phi(\mathbf{x}, t)$ and $\delta\mathbf{B}(\mathbf{x}, t) \simeq 0$. Perturbed quantities are expressed as $\delta\phi(r, z, t) = \delta\phi(r) \exp(ik_z z - i\omega t)$, where k_z is the axial wavenumber, and $Im\omega > 0$ corresponds to instability (temporal growth). Using the same assumptions as in Sec. II, without presenting algebraic details [73] the cold-fluid-Poisson equations for the beam-plasma system can be expressed as

$$\frac{1}{r} \frac{\partial}{\partial r} \left[r \left(1 - \sum_{j=b,e,i} \frac{\omega_{pj}^2(r)/\gamma_j^2}{(\omega - k_z V_{zj})^2} \right) \frac{\partial}{\partial r} \delta\phi \right] - k_z^2 \left(1 - \sum_{j=b,e,i} \frac{\omega_{pj}^2(r)/\gamma_j^2}{(\omega - k_z V_{zj})^2} \right) \delta\phi = 0, \quad (42)$$

where $\omega_{pj}^2(r) = 4\pi n_j^0(r) e_j^2 / \gamma_j m_j$, $V_{zj} = \beta_j c$, $\gamma_j = (1 - \beta_j^2)^{-1/2}$, and the notation is the same as in Secs. II and III.

The electrostatic eigenvalue equation (42) can be used to calculate the complex eigenfrequency ω and eigenfunction $\delta\phi(r)$ for a wide range of density profiles $n_j^0(r)$. For present purposes, we specialize to the case of the step-function density profiles considered in Sec. III and illustrated in Fig. 1. For the choice of profiles in Fig. 1 and Eqs. (17) and (18), Eq. (42) can be solved exactly inside the beam-plasma system ($0 \leq r < r_b$; Region I) and outside the beam ($r_b < r \leq r_w$; Region II) subject to the requirements that $\delta\phi(r)$ be regular at $r = 0$ and satisfy $\delta\phi(r = r_w) = 0$ at the conducting wall. Without presenting algebraic details, integrating Eq. (42) across the beam surface

at $r = r_b$ then gives the dispersion relation

$$\left[1 - \sum_{j=b,e,i} \frac{\hat{\omega}_{pj}^{i2}/\gamma_j^2}{(\omega - k_z V_{zj})^2} \right] = -\frac{1}{g_0} \left[1 - \sum_{j=e,i} \frac{\hat{\omega}_{pj}^{02}}{\omega^2} \right], \quad (43)$$

where $\hat{\omega}_{pj}^{i2} = 4\pi\hat{n}_j^i e_j^2 / \gamma_j m_j$ inside the beam, and $\hat{\omega}_{pj}^{02} = 4\pi\hat{n}_j^0 e_j^2 / m_j$ outside the beam. Similar to Sec. III, we assume $\beta_e = 0 = \beta_i$ in the region outside the beam, $\beta_i = 0$ inside the beam, and that β_e is related to β_b by the current neutrality condition in Eq. (38) inside the beam. In Eq. (43), g_0 is the geometric factor defined by

$$g_0 = -\frac{I'_0(k_z r_b) [I_0(k_z r_b) K_0(k_z r_w) - K_0(k_z r_b) I_0(k_z r_w)]}{I_0(k_z r_b) [I'_0(k_z r_b) K_0(k_z r_w) - K'_0(k_z r_b) I_0(k_z r_w)]}, \quad (44)$$

where $I'_0(x)$ denotes $(d/dx)I_0(x)$, etc., where $r_b \neq r_w$ is assumed.

It is convenient to introduce the quantity s_0 defined by

$$s_0 = \frac{g_0}{1 + g_0}. \quad (45)$$

Some straightforward algebra then shows that the dispersion relation (43) can be expressed in the equivalent form

$$D(k_z, \omega) = 1 - s_0 \sum_{j=b,e,i} \frac{\hat{\omega}_{pj}^{i2}/\gamma_j^2}{(\omega - k_z V_{zj})^2} - (1 - s_0) \sum_{j=e,i} \frac{\hat{\omega}_{pj}^{02}}{\omega^2} = 0, \quad (46)$$

where s_0 is given (exactly) by

$$s_0 = k_z r_b I'_0(k_z r_b) I_0(k_z r_b) \left[\frac{K_0(k_z r_b)}{I_0(k_z r_b)} - \frac{K_0(k_z r_w)}{I_0(k_z r_w)} \right], \quad (47)$$

for $r_b \neq r_w$. In obtaining Eq. (47) from Eqs. (44) and (45), use has been made of the Wronskian identity $K_0(x)I'_0(x) - I_0(x)K'_0(x) = 1/x$. Note from Eq. (47) that the geometric factor s_0 exhibits a strong dependence on k_z with

$$s_0 \simeq \frac{1}{2} k_z^2 r_b^2 \ell n \left(\frac{r_w}{r_b} \right) \quad \text{for } k_z^2 r_w^2 \ll 1, \quad (48)$$

and

$$s_0 \simeq \frac{1}{2} \quad \text{for } k_z^2 r_b^2 \gg 1. \quad (49)$$

Due to the geometric factors s_0 and $1 - s_0$ in Eq. (46), the detailed properties of the two-stream instability calculated from Eq. (46) differ substantially from the infinite beam-plasma results. However, several interesting features of Eq. (46) are qualitatively evident. First, in the absence of plasma outside the beam-plasma channel ($\hat{\omega}_{pj}^{02} = 0$), the channel electrons undergo unstable

two-stream interactions with both the beam ions and the channel plasma ions. Second, when there is plasma outside the beam-plasma channel ($\hat{\omega}_{pj}^{02} \neq 0$), the channel electrons can undergo a strong unstable two-stream interaction with the plasma electrons outside the channel.

We now present detailed two-stream instability results obtained from Eq. (46) for system parameters similar to those chosen in Figs. 6–9 in the analysis of the Weibel instability in Sec. III.

A. Beam-Plasma-Filled Waveguide ($r_b = r_w$)

Illustrative stability results obtained from Eq. (42) are shown in Figs. 10 and 11 for the case of a beam-plasma-filled waveguide ($r_b = r_w$). Here, we assume a cesium ion beam with $\beta_b = 0.2$ and $Z_b = 1$ propagating through background argon plasma with $Z_i = 1$ and $\beta_i = 0$. Assuming $\hat{n}_b^i = \hat{n}_e^i/2 = \hat{n}_i^i$, the current neutralization condition in Eq. (38) gives $\beta_e = 0.1$. For a beam-plasma-filled waveguide ($r_b = r_w$), the dispersion relation obtained from Eq. (42) is identical to Eq. (46) with $s_0 = 1$. Furthermore, the dispersion relation (46) has two unstable branches corresponding to the interaction of the plasma electrons with the beam ions, and the interaction of the plasma electrons with the plasma ions. The unstable branches in Figs. 10 and 11 correspond to the interaction of the plasma electrons with the plasma ions. Figures 10 and 11 show plots of (a) the normalized growth $(Im\omega)/\hat{\omega}_{pe}^i$ and (b) the real oscillation frequency $(Re\omega)/\hat{\omega}_{pe}^i$ versus $k_z r_b$ for the two cases corresponding to $\hat{\omega}_{pe}^i r_b/c = 1/3$ (Fig. 10), and $\hat{\omega}_{pe}^i r_b/c = 3$ (Fig. 11). Note from Figs. 10 and 11 that the two-stream growth rate is strongly peaked as a function of $k_z r_b$. For the choice of system parameters in Fig. 11, the value of $k_z = k_{zm}$ at maximum growth rate satisfies $k_{zm}^2 r_b^2 \gg 1$. The maximum growth rate $(Im\omega)_{max}$ and value of k_{zm} in Fig. 11 is given to excellent approximation by the analytical estimates

$$\begin{aligned} (Im\omega)_{max} &\simeq \left(\frac{3s_0}{4}\right)^{1/2} \left(\frac{\hat{\omega}_{pi}^{i2}}{2\hat{\omega}_{pe}^{i2}}\right)^{1/3} \hat{\omega}_{pe}^i, \\ |k_{zm}|r_b &\simeq (s_0)^{1/2} \frac{\hat{\omega}_{pe}^i r_b}{c} \frac{1}{|\beta_i - \beta_e|}, \end{aligned} \quad (50)$$

where $\beta_i = 0$ is assumed and $s_0 = 1$. Equation (50) pertains to the unstable plasma electron-plasma ion two-stream solution to Eq. (46). For the unstable plasma electron-beam ion solution to Eq. (46), the estimates are similar to those in Eq. (50) with $\hat{\omega}_{pi}^i$ replaced by $\hat{\omega}_{pb}^i$, and $\beta_i - \beta_e$ replaced by $\beta_b - \beta_e$.

B. Vacuum Region Outside of Beam-Plasma Channel ($r_b < r_w$; $\hat{n}_j^0 = 0, j = e, i$).

We now consider the case where there is a vacuum region outside the beam-plasma channel, i.e., $r_b < r_w$ and $\hat{n}_j^0 = 0, j = e, i$. Figures 12 and 13 show plots of (a) the normalized growth $(Im\omega)/\hat{\omega}_{pe}^i$ and (b) the real oscillation frequency $(Re\omega)/\hat{\omega}_{pe}^i$ versus $k_z r_b$ for the two cases corresponding to $\hat{\omega}_{pe}^i r_b/c = 1/3$ (Fig. 12), and $\hat{\omega}_{pe}^i r_b/c = 3$ (Fig. 13) and the choice of system parameters $r_w = 3r_b$, $\beta_b = 0.2$, $\beta_e = 0.1$ and $\hat{n}_b^i = \hat{n}_e^i/2 = \hat{n}_i^i$. Note from Figs. 12 and 13 that the signature of the instability growth rate for the case of a vacuum region outside the beam-plasma channel is qualitatively similar to that in Figs. 10 and 11 for the case of a beam-plasma-filled waveguide. The most unstable branch plotted in Figs. 12 and 13 corresponds to the interaction of the plasma electrons with the plasma ions. The maximum growth rate $(Im\omega)_{max}$ and value of k_{zm} in Fig. 13 is given to excellent approximation by the analytical estimates in Eq. (50) with $s_0 \simeq 1/2$.

C. Plasma Outside of Beam-Plasma Channel ($r_b < r_w$; $\hat{n}_j^0 \neq 0, j = e, i$)

We now consider the dispersion relation (46) for the case where there is plasma outside the beam-plasma channel, i.e., $r_b < r_w$ and $\hat{n}_j^0 \neq 0, j = e, i$. Typical numerical solutions to Eq. (46) for the most unstable branch are illustrated in Figs. 14 and 15 for the choice of system parameters $r_w = 3r_b$. Shown in Figs. 14 and 15 are plots of (a) the normalized growth rate $Im\omega/\hat{\omega}_{pe}^i$ and (b) the real oscillation frequency $(Re\omega)/\hat{\omega}_{pe}^i$ versus $k_z r_b$ for the two cases corresponding to $\hat{\omega}_{pe}^i r_b/c = 1/3$ (Fig. 14), and $\hat{\omega}_{pe}^i r_b/c = 3$ (Fig. 15). Comparing Fig. 14 with Fig. 12, and Fig. 15 with Fig. 13, it is evident that the inclusion of plasma outside the beam-plasma channel significantly change the instability growth rate relative to the case where there is vacuum outside the beam-plasma channel. In the absence of plasma outside the beam-plasma channel ($\hat{\omega}_{pj}^{o2} = 0$), the channel electrons undergo unstable two-stream interactions with both the beam ions and the channel plasma ions. When there is plasma outside the beam-plasma channel ($\hat{\omega}_{pj}^{o2} \neq 0$), the channel electrons can undergo a strong unstable two-stream interaction with the plasma electrons outside the channel.

V. CONCLUSIONS

In this paper we have made use of a macroscopic cold-fluid model to investigate detailed properties of the multi-species electromagnetic Weibel instability (Sec. III) and electrostatic two-stream instability (Sec. IV) for an intense ion beam propagating through a background plasma that provides complete charge and current neutralization. Detailed growth-rate properties have been cal-

culated for a wide range of system parameters.

Acknowledgments

This research was supported by the U.S. Department of Energy.

-
- [1] R. C. Davidson and H. Qin, *Physics of Intense Charged Particle Beams in High Energy Accelerators* (World Scientific, Singapore, 2001), and references therein.
 - [2] M. Reiser, *Theory and Design of Charged Particle Beams* (Wiley, New York, 1994).
 - [3] J. D. Lawson, *The Physics of Charged-Particle Beams* (Oxford Science Publications, New York, 1988).
 - [4] A. W. Chao, *Physics of Collective Beam Instabilities in High Energy Accelerators* (Wiley, New York, 1993).
 - [5] D. A. Edwards and M. J. Syphers, *An Introduction to the Physics of High-Energy Accelerators* (Wiley, New York, 1993).
 - [6] I. M. Kapchinskij and V. V. Vladimirkij, in *Proceedings of the International Conference on High Energy Accelerators and Instrumentation* (CERN Scientific Information Service, Geneva, 1959), p. 274.
 - [7] R. L. Gluckstern, in *Proceedings of the 1970 Proton Linear Accelerator Conference, Batavia, IL*, edited by M. R. Tracy (National Accelerator Laboratory, Batavia, IL, 1971), p. 811.
 - [8] T. -S. Wang and I. Smith, *Part. Accel.* **12**, 247 (1982).
 - [9] J. Hofmann, L. J. Laslett, L. Smith, and I. Haber, *Part. Accel.* **13**, 145 (1983).
 - [10] J. Struckmeier, J. Klabunde, and M. Reiser, *Part. Accel.* **15**, 47 (1984).
 - [11] I. Hofmann and J. Struckmeier, *Part. Accel.* **21**, 69 (1987).
 - [12] J. Struckmeier and I. Hofmann, *Part. Accel.* **39**, 219 (1992).
 - [13] N. Brown and M. Reiser, *Phys. Plasmas* **2**, 965 (1995).
 - [14] R. C. Davidson and H. Qin, *Phys. Rev. ST Accel. Beams* **2**, 114401 (1999).
 - [15] R. L. Gluckstern, W. -H. Cheng, and H. Ye, *Phys. Rev. Lett.* **75**, 2835 (1995).
 - [16] R. C. Davidson and C. Chen, *Part. Accel.* **59**, 175 (1998).
 - [17] C. Chen, R. Pakter, and R. C. Davidson, *Phys. Rev. Lett.* **79**, 225 (1997).
 - [18] C. Chen and R. C. Davidson, *Phys. Rev. E* **49**, 5679 (1994).
 - [19] R. C. Davidson, W. W. Lee, and P. Stoltz, *Phys. Plasmas* **5**, 279 (1998).
 - [20] R. C. Davidson, *Phys. Rev. Lett.* **81**, 991 (1998).
 - [21] R. C. Davidson, *Phys. Plasmas* **5**, 3459 (1998).
 - [22] P. Stoltz, R. C. Davidson, and W. W. Lee, *Phys. Plasmas* **6**, 298 (1999).
 - [23] W. W. Lee, Q. Qian, and R. C. Davidson, *Phys. Lett. A* **230**, 347 (1997).
 - [24] Q. Qian, W. W. Lee, and R. C. Davidson, *Phys. Plasmas* **4**, 1915 (1997).

- [25] S. I. Tzenov and R. C. Davidson, *Phys. Rev. ST Accel. Beams* **5**, 021001 (2002).
- [26] R. C. Davidson and H. Qin, *Phys. Rev. ST Accel. Beams* **4**, 104401 (2001).
- [27] R. C. Davidson, H. Qin, and P. J. Channell, *Phys. Rev. ST Accel. Beams* **2**, 074401 (1999); **3**, 029901 (2000).
- [28] R. C. Davidson, A. Friedman, C. M. Celata, D. R. Welch, et al., *Laser and Particle Beams* **20**, 377 (2002).
- [29] E. G. Harris, *Phys. Rev. Lett.* **2**, 34 (1959).
- [30] E. A. Startsev, R. C. Davidson and H. Qin, *Physics of Plasmas* **9**, 3138 (2002).
- [31] E. A. Startsev, R. C. Davidson and H. Qin, *Laser and Particle Beams* **20**, 585 (2002).
- [32] E. A. Startsev, R. C. Davidson and H. Qin, *Physical Review Special Topics on Accelerators and Beams* **6**, 084401 (2003).
- [33] R. A. Kishek, P. G. O'Shea, and M. Reiser, *Phys. Rev. Lett.* **85**, 4514 (2000).
- [34] J. Haber, A. Friedman, D. P. Grote, S. M. Lund, and R. A. Kishek, *Phys. Plasmas* **6**, 2254 (1999).
- [35] A. Friedman, D. P. Grote, and I. Haber, *Phys. Fluids B* **4**, 2203 (1992).
- [36] E. S. Weibel, *Phys. Rev. Lett.* **2**, 83 (1959).
- [37] E. A. Startsev and R. C. Davidson, *Physics of Plasmas* **10**, 4829 (2003).
- [38] R. C. Davidson, D. A. Hammer, I. Haber and C. E. Wagner, *Phys. Fluids* **15**, 317 (1972).
- [39] R. Lee and M. Lampe, *Phys. Rev. Lett.* **31**, 1390 (1973).
- [40] C. A. Kapetanacos, *Appl. Phys. Lett.* **25**, 484 (1974).
- [41] M. Honda, J. Meyer-ter-Vehn, A. Pukhov, *Phys. Rev. Lett.* **85**, 2128 (2000).
- [42] V. K. Neil and A. M. Sessler, *Rev. Sci. Instr.* **36**, 429 (1965).
- [43] E. P. Lee, in *Proceedings of the 1981 Linear Accelerator Conference*, Los Alamos National Laboratory Report LA-9234-C, pp. 263–265.
- [44] E. P. Lee, *Particle Accelerators* **37**, 307 (1992).
- [45] R. C. Davidson, H. Qin and G. Shvets, *Physical Review Special Topics on Accelerators and Beams* **6**, 104402 (2003).
- [46] D. Neuffer, B. Colton, D. Fitzgerald, T. Hardek, R. Hutson, R. Macek, M. Plum, H. Thiessen, and T. S. Wang, *Nucl. Strum. Methods Phys. Res.* **A321**, 1 (1992).
- [47] R. J. Macek, et al., *Proceedings of the 2001 Particle Accelerator Conference* **1**, 688 (2001).
- [48] R. C. Davidson, H. Qin, and T. -S. Wang, *Physics Letters* **A252**, 213 (1999).
- [49] R. C. Davidson, H. Qin, P. H. Stoltz, and T. -S. Wang, *Physical Review Special Topics on Accelerators and Beams* **2**, 054401 (1999).
- [50] R. C. Davidson and H. Qin, *Physics Letters* **A270**, 177 (2000).
- [51] H. Qin, R. C. Davidson and W. W. Lee, *Physical Review Special Topics on Accelerators and Beams* **3**, 084401 (2000); **3**, 109901 (2000).
- [52] R. C. Davidson and H. S. Uhm, *Physics Letters* **A285**, 88 (2001).
- [53] H. Qin, R. C. Davidson, E. A. Startsev and W. W. Lee, *Laser and Particle Beams* **21**, 21 (2003).

- [54] T. -S. Wang, P. J. Channell, R. J. Macek, and R. C. Davidson, *Physical Review Special Topics on Accelerators and Beams* **6**, 014204 (2003).
- [55] H. Qin, E. A. Startsev and R. C. Davidson, *Physical Review Special Topics on Accelerators and Beams* **6**, 014401 (2003).
- [56] H. Qin, *Physics of Plasmas* **10**, 2708 (2003).
- [57] E. P. Lee, *Phys. Fluids* **21**, 1327 (1978).
- [58] E. J. Lauer, R. J. Briggs, T. J. Fesendon, R. E. Hester, and E. P. Lee, *Phys. Fluids* **21**, 1344 (1978).
- [59] M. N. Rosenbluth, *Phys. Fluids* **3**, 932 (1960).
- [60] H. S. Uhm and M. Lampe, *Phys. Fluids* **23**, 1574 (1980).
- [61] H. S. Uhm and M. Lampe, *Phys. Fluids* **24**, 1553 (1981).
- [62] R. F. Fernsler, S. P. Slinker, M. Lampe, and R. F. Hubbard, *Phys. Plasmas* **2**, 4338 (1995), and references therein.
- [63] H. S. Uhm and R. C. Davidson, *Physical Review Special Topics on Accelerators and Beams* **6**, 034204 (2003).
- [64] H. S. Uhm, R. C. Davidson and I. D. Kaganovich, *Physics of Plasmas* **8**, 4637 (2001).
- [65] G. Joyce and M. Lampe, *Phys. Fluids* **26**, 3377 (1983).
- [66] H. S. Uhm and R. C. Davidson, *Phys. Fluids* **23**, 1586 (1980).
- [67] I. D. Kaganovich, G. Shvets, E. Startsev and R. C. Davidson, *Physics of Plasmas* **8**, 4180 (2001).
- [68] I. Kaganovich, E. A. Startsev and R. C. Davidson, *Laser and Particle Beams* **20**, 497 (2002).
- [69] D. V. Rose, P. F. Ottinger, D. R. Welch, B. V. Oliver and C. L. Olson, *Phys. Plasmas* **6**, 4094 (1999).
- [70] D. R. Welch, D. V. Rose, B. V. Oliver, T. C. Genoni, C. L. Olson and S. S. Yu, *Phys. Plasmas* **9**, 2344 (2002).
- [71] R. C. Davidson, *Physics of Nonneutral Plasmas* (World Scientific, 2001).
- [72] See, for example, pp. 272-276 of Ref. 71.
- [73] See, for example, Sec. 9.5 of Ref. 1.

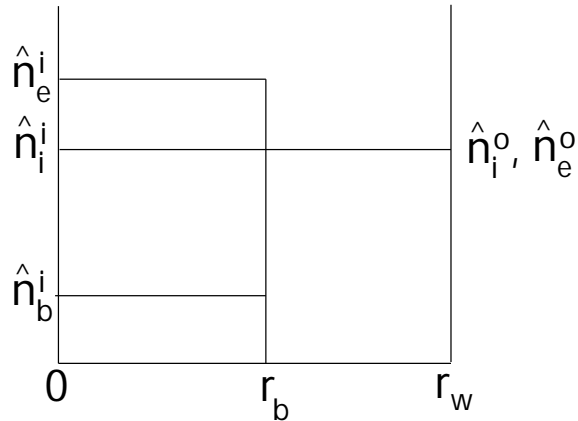


FIG. 1: Schematics of the density profiles of the beam ions (\hat{n}_b^i) and the plasma ions and electrons inside (\hat{n}_i^i and \hat{n}_e^i) and outside (\hat{n}_i^o and \hat{n}_e^o) the beam.

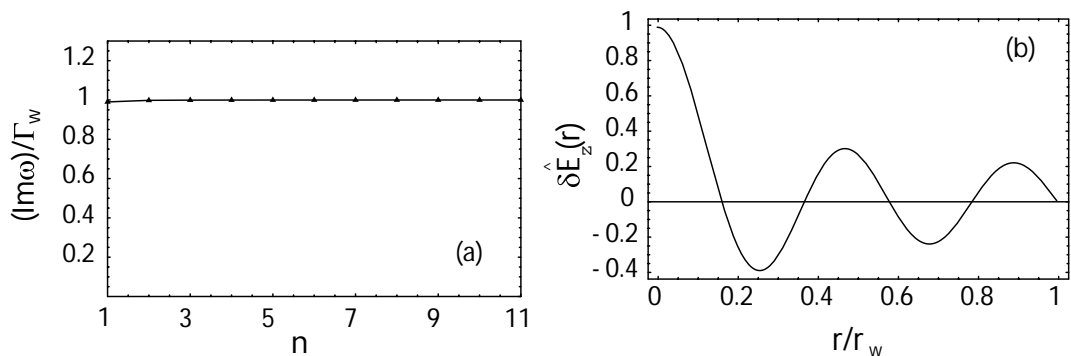


FIG. 2: Plots of (a) Weibel instability growth rate $(Im\omega)/\Gamma_w$ versus mode radial number n , and (b) eigenfunction $\delta\hat{E}_z(r)$ versus r/r_w for $n = 5$ obtained from Eq. (26). System parameters are $r_b = r_w$, $\beta_b = 0.2$, $\beta_e = 0.1$, $\hat{n}_i^i = \hat{n}_e^i/2 = \hat{n}_b^i$, and $\Omega_p^i r_b/c = 1/3$.

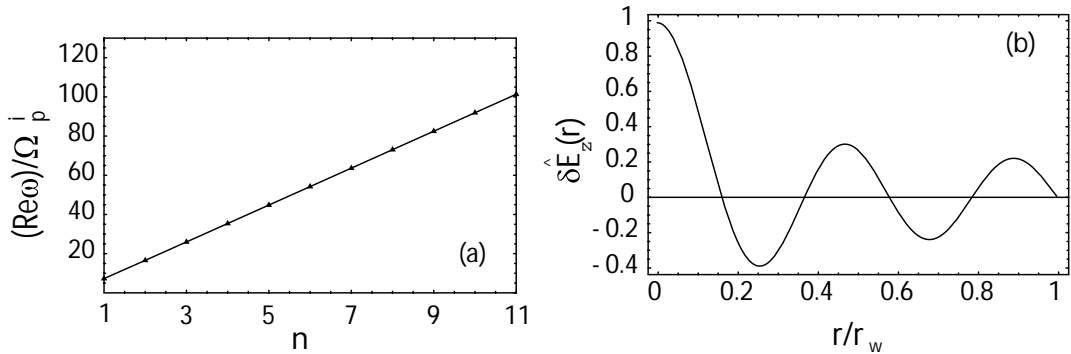


FIG. 3: Plots of (a) stable fast-wave oscillation frequency $(Re\omega)/\Omega_p^i$ versus radial mode number n , and (b) eigenfunction $\delta\hat{E}_z(r)$ versus r/r_w for $n = 5$ obtained from Eq. (26). System parameters are $r_b = r_w$, $\beta_b = 0.2$, $\beta_e = 0.1$, $\hat{n}_i^i = \hat{n}_e^i/2 = \hat{n}_b^i$, and $\Omega_p^i r_b/c = 1/3$.

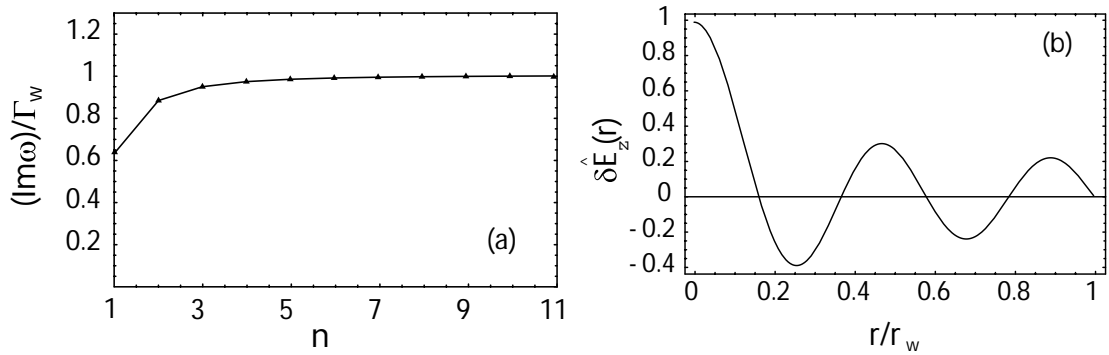


FIG. 4: Plots of (a) Weibel instability growth rate $(Im\omega)/\Gamma_w$ versus radial mode number n , and (b) eigenfunction $\delta\hat{E}_z(r)$ versus r/r_w for $n = 5$ obtained from Eq. (26). System parameters are $r_b = r_w$, $\beta_b = 0.2$, $\beta_e = 0.1$, $\hat{n}_i^i = \hat{n}_e^i/2 = \hat{n}_b^i$, and $\Omega_p^i r_b/c = 3$.

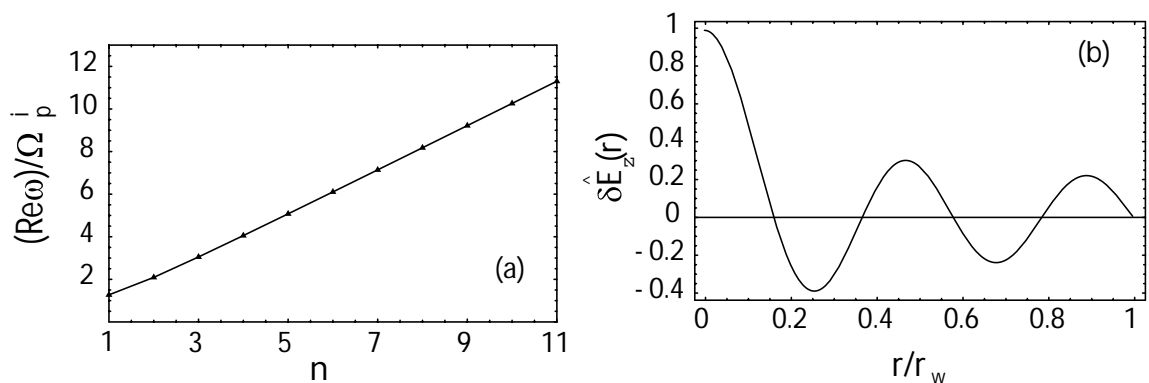


FIG. 5: Plots of (a) stable fast-wave oscillation frequency $(Re\omega)/\Omega_p^i$ versus radial mode number n , and (b) eigenfunction $\delta\hat{E}_z(r)$ versus r/r_w for $n = 5$ obtained from Eq. (26). System parameters are $r_b = r_w$, $\beta_b = 0.2$, $\beta_e = 0.1$, $\hat{n}_i^i = \hat{n}_e^i/2 = \hat{n}_b^i$, and $\Omega_p^i r_b/c = 3$.

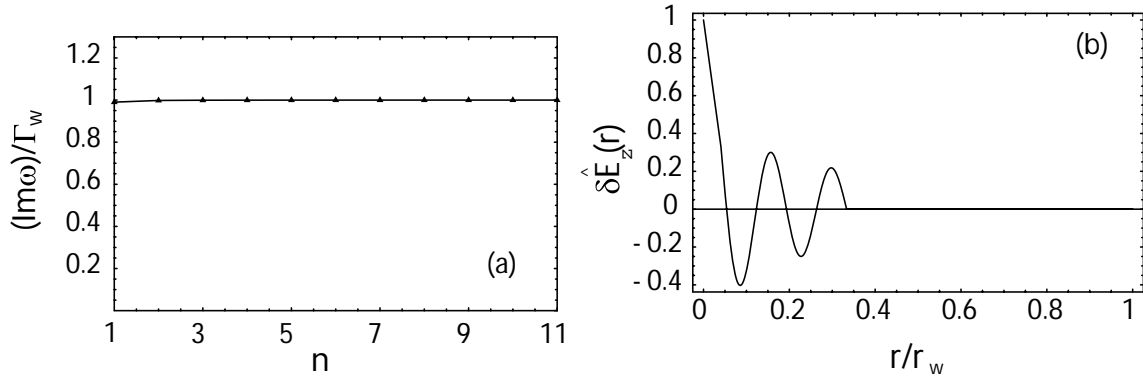


FIG. 6: Plots of (a) Weibel instability growth rate $(Im\omega)/\Gamma_w$ versus radial mode number n , and (b) eigenfunction $\delta\hat{E}_z(r)$ versus r/r_w for $n = 5$ obtained from Eq. (26). System parameters are $r_b = r_w/3$, $\beta_b = 0.2$, $\beta_e = 0.1$, $\hat{n}_i^i = \hat{n}_e^i/2 = \hat{n}_b^i$, $\Omega_p^i r_b/c = 1/3$ and $\Omega_p^0 = 0$.

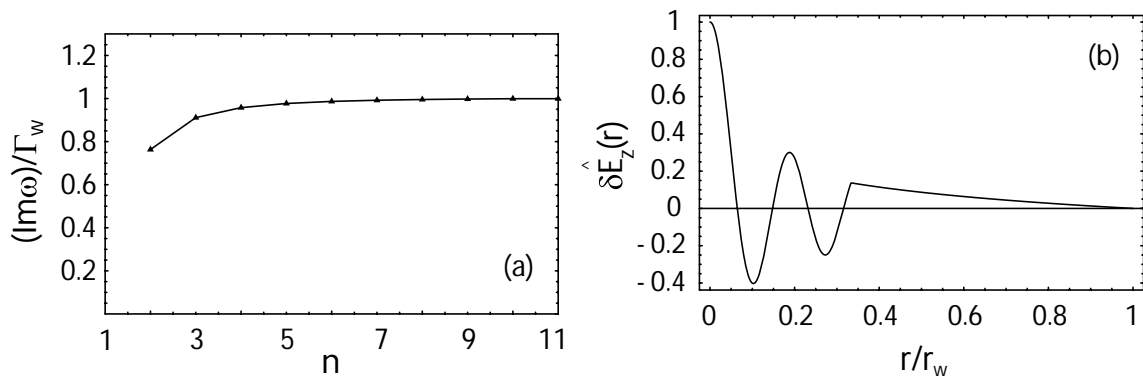


FIG. 7: Plots of (a) Weibel instability growth rate $(Im\omega)/\Gamma_w$ versus radial mode number n , and (b) eigenfunction $\delta\hat{E}_z(r)$ versus r/r_w for $n = 5$ obtained from Eq. (26). System parameters are $r_b = r_w/3$, $\beta_b = 0.2$, $\beta_e = 0.1$, $\hat{n}_i^i = \hat{n}_e^i/2 = \hat{n}_b^i$, $\Omega_p^i r_b/c = 3$ and $\Omega_p^0 = 0$.

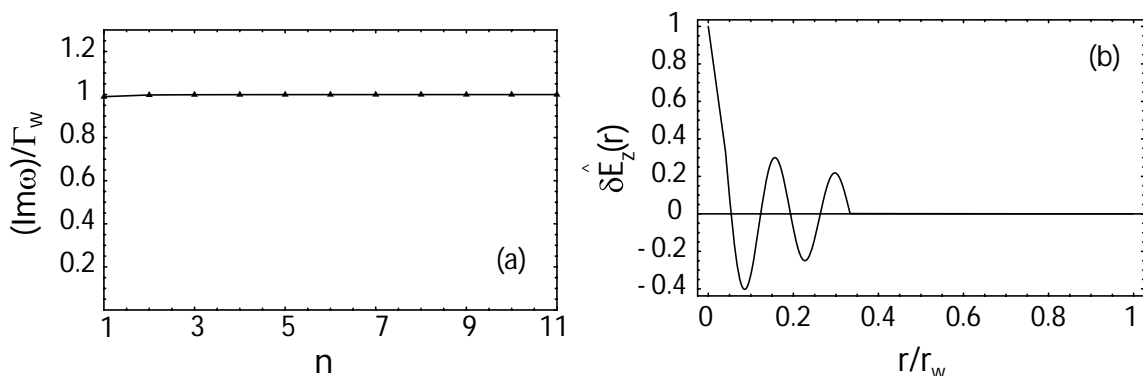


FIG. 8: Plots of (a) Weibel instability growth rate $(Im\omega)/\Gamma_w$ versus radial mode number n , and (b) eigenfunction $\delta\hat{E}_z(r)$ versus r/r_w for $n = 5$ obtained from Eq. (26). System parameters are $r_b = r_w/3$, $\beta_b = 0.2$, $\beta_e = 0.1$, $\hat{n}_i^i = \hat{n}_e^i/2 = \hat{n}_b^i = \hat{n}_e^o = \hat{n}_i^o$, $\Omega_p^i r_b/c = 1/3$.

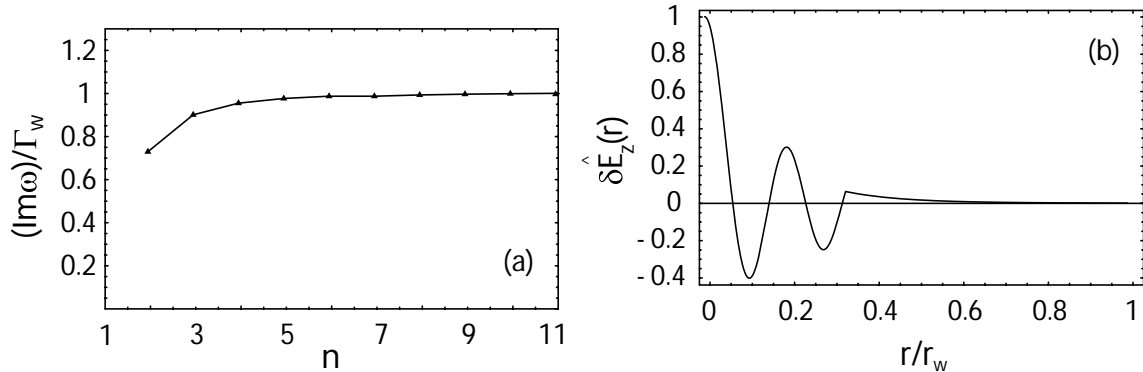


FIG. 9: Plots of (a) Weibel instability growth rate $(Im\omega)/\Gamma_w$ versus radial mode number n , and (b) eigenfunction $\delta\hat{E}_z(r)$ versus r/r_w for $n = 5$ obtained from Eq. (26). System parameters are $r_b = r_w/3$, $\beta_b = 0.2$, $\beta_e = 0.1$, $\hat{n}_i^i = \hat{n}_e/2 = \hat{n}_b^i = \hat{n}_e^o = \hat{n}_i^o$, $\Omega_p^i r_b/c = 3$.

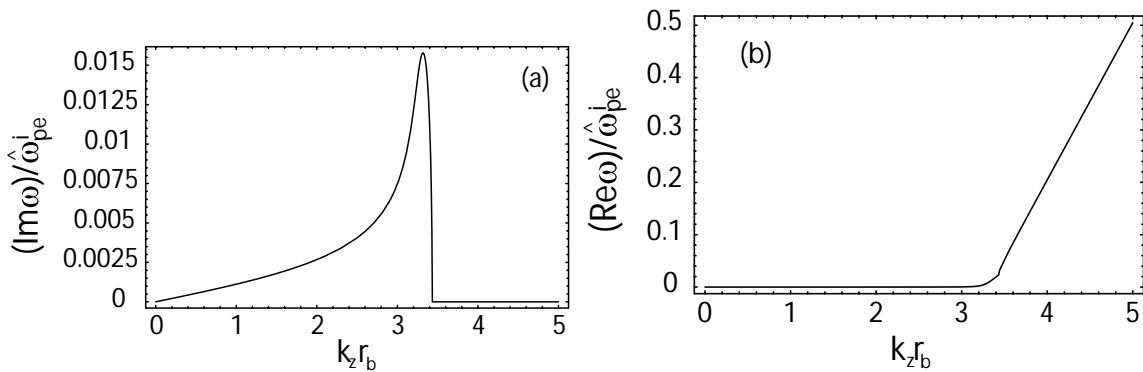


FIG. 10: Plots of (a) $(Im\omega)/\hat{\omega}_{pe}^i$ and (b) $(Re\omega)/\hat{\omega}_{pe}^i$ versus $k_z r_b$ calculated from the two-stream dispersion relation (46) for $r_b = r_w$, $\beta_b = 0.2$, $\beta_e = 0.1$ and $\hat{\omega}_{pe}^i r_b/c = 1/3$.

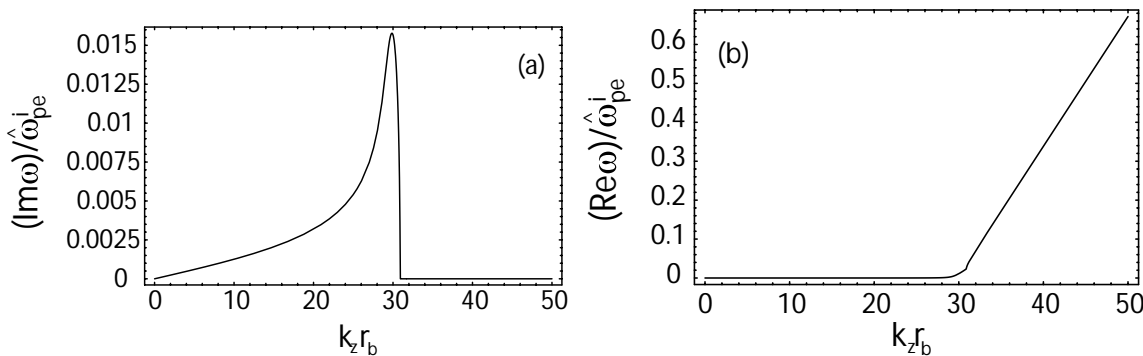


FIG. 11: Plots of (a) $(Im\omega)/\hat{\omega}_{pe}^i$ and (b) $(Re\omega)/\hat{\omega}_{pe}^i$ versus $k_z r_b$ calculated from the two-stream dispersion relation (46) for $r_b = r_w$, $\beta_b = 0.2$, $\beta_e = 0.1$ and $\hat{\omega}_{pe}^i r_b/c = 3$.

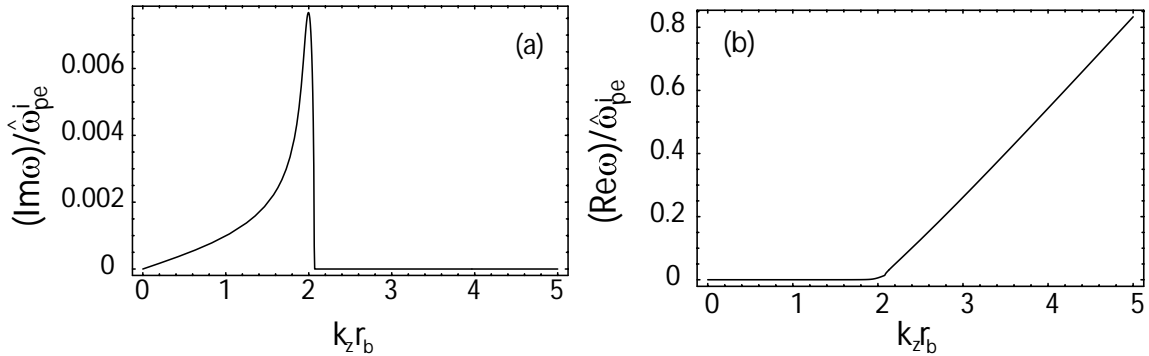


FIG. 12: Plots of (a) $(Im\omega)/\hat{\omega}_{pe}^i$ and (b) $(Re\omega)/\hat{\omega}_{pe}^i$ versus $k_z r_b$ calculated from the two-stream dispersion relation (46) for $r_b = r_w/3$, $\beta_b = 0.2$, $\beta_e = 0.1$ and $\hat{\omega}_{pe}^i r_b/c = 1/3$ in the absence of plasma outside the beam-plasma channel.

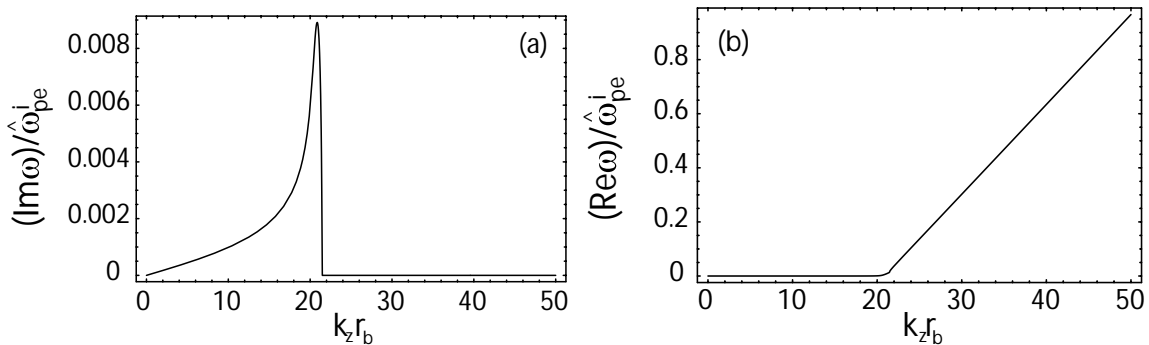


FIG. 13: Plots of (a) $(Im\omega)/\hat{\omega}_{pe}^i$ and (b) $(Re\omega)/\hat{\omega}_{pe}^i$ versus $k_z r_b$ calculated from the two-stream dispersion relation (46) for $r_b = r_w/3$, $\beta_b = 0.2$, $\beta_e = 0.1$ and $\hat{\omega}_{pe}^i r_b/c = 3$ in the absence of plasma outside the beam-plasma channel.

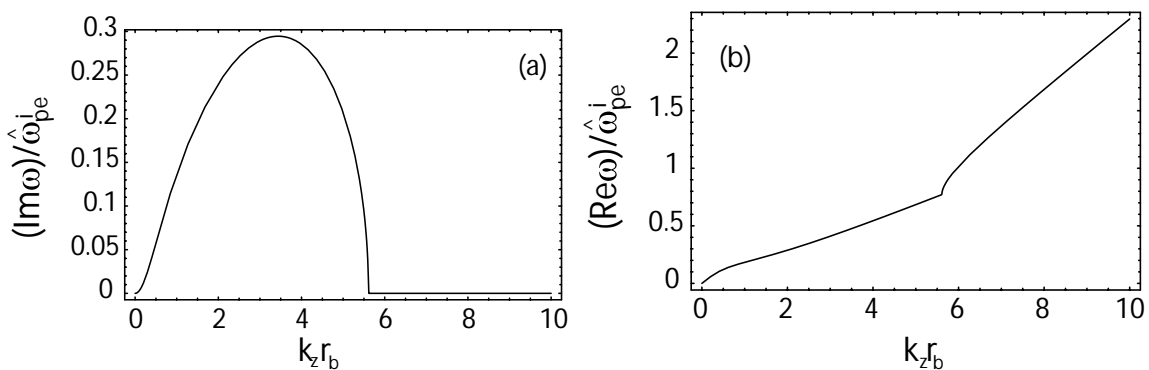


FIG. 14: Plots of (a) $(Im\omega)/\hat{\omega}_{pe}^i$ and (b) $(Re\omega)/\hat{\omega}_{pe}^i$ versus $k_z r_b$ calculated from the two-stream dispersion relation (46) for $r_b = r_w/3$, $\beta_b = 0.2$, $\beta_e = 0.1$ and $\hat{\omega}_{pe}^i r_b/c = 1/3$ including plasma outside the beam-plasma channel with $n_i^o = n_e^o = n_i^i$.

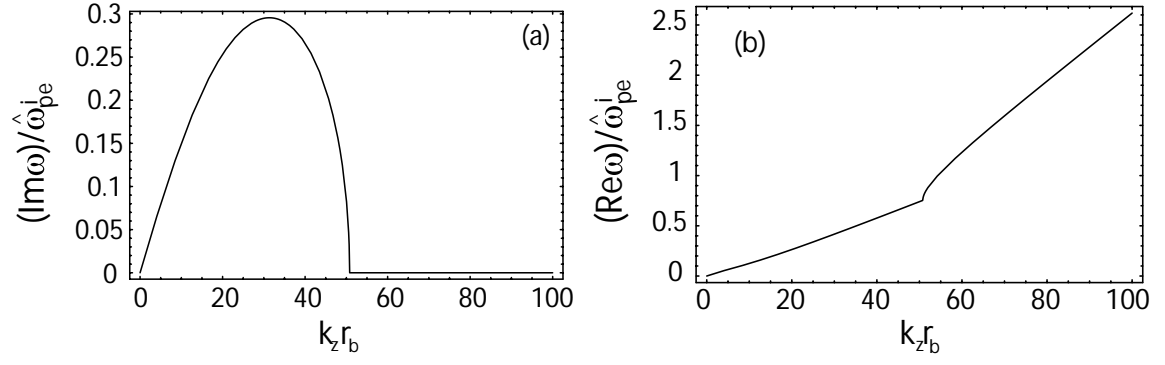


FIG. 15: Plots of (a) $(Im\omega)/\hat{\omega}_{pe}^i$ and (b) $(Re\omega)/\hat{\omega}_{pe}^i$ versus $k_z r_b$ calculated from the two-stream dispersion relation (46) for $r_b = r_w/3$, $\beta_b = 0.2$, $\beta_e = 0.1$ and $\hat{\omega}_{pe}^i r_b/c = 3$ including plasma outside the beam-plasma channel with $n_i^o = n_e^o = n_i^i$.

External Distribution

Plasma Research Laboratory, Australian National University, Australia
Professor I.R. Jones, Flinders University, Australia
Professor João Canalle, Instituto de Fisica DEQ/IF - UERJ, Brazil
Mr. Gerson O. Ludwig, Instituto Nacional de Pesquisas, Brazil
Dr. P.H. Sakanaka, Instituto Fisica, Brazil
The Librarian, Culham Laboratory, England
Mrs. S.A. Hutchinson, JET Library, England
Professor M.N. Bussac, Ecole Polytechnique, France
Librarian, Max-Planck-Institut für Plasmaphysik, Germany
Jolan Moldvai, Reports Library, Hungarian Academy of Sciences, Central Research Institute
for Physics, Hungary
Dr. P. Kaw, Institute for Plasma Research, India
Ms. P.J. Pathak, Librarian, Institute for Plasma Research, India
Ms. Clelia De Palo, Associazione EURATOM-ENEA, Italy
Dr. G. Grosso, Instituto di Fisica del Plasma, Italy
Librarian, Naka Fusion Research Establishment, JAERI, Japan
Library, Laboratory for Complex Energy Processes, Institute for Advanced Study,
Kyoto University, Japan
Research Information Center, National Institute for Fusion Science, Japan
Dr. O. Mitarai, Kyushu Tokai University, Japan
Dr. Jiengang Li, Institute of Plasma Physics, Chinese Academy of Sciences,
People's Republic of China
Professor Yuping Huo, School of Physical Science and Technology, People's Republic of China
Library, Academia Sinica, Institute of Plasma Physics, People's Republic of China
Librarian, Institute of Physics, Chinese Academy of Sciences, People's Republic of China
Dr. S. Mirnov, TRINITI, Troitsk, Russian Federation, Russia
Dr. V.S. Strelkov, Kurchatov Institute, Russian Federation, Russia
Professor Peter Lukac, Katedra Fyziky Plazmy MFF UK, Mlynska dolina F-2,
Komenskeho Univerzita, SK-842 15 Bratislava, Slovakia
Dr. G.S. Lee, Korea Basic Science Institute, South Korea
Institute for Plasma Research, University of Maryland, USA
Librarian, Fusion Energy Division, Oak Ridge National Laboratory, USA
Librarian, Institute of Fusion Studies, University of Texas, USA
Librarian, Magnetic Fusion Program, Lawrence Livermore National Laboratory, USA
Library, General Atomics, USA
Plasma Physics Group, Fusion Energy Research Program, University of California
at San Diego, USA
Plasma Physics Library, Columbia University, USA
Alkesh Punjabi, Center for Fusion Research and Training, Hampton University, USA
Dr. W.M. Stacey, Fusion Research Center, Georgia Institute of Technology, USA
Dr. John Willis, U.S. Department of Energy, Office of Fusion Energy Sciences, USA
Mr. Paul H. Wright, Indianapolis, Indiana, USA

The Princeton Plasma Physics Laboratory is operated
by Princeton University under contract
with the U.S. Department of Energy.

Information Services
Princeton Plasma Physics Laboratory
P.O. Box 451
Princeton, NJ 08543

Phone: 609-243-2750
Fax: 609-243-2751
e-mail: pppl_info@pppl.gov
Internet Address: <http://www.pppl.gov>